Crystallization and melting behavior of isotactic polypropylene nucleated with individual and compound nucleating agents

**Zhiyong Wei · Wanxi Zhang · Guangyi Chen ·
Jicai Liang · Shu Yang · Pei Wang ·
Lian Liu**

Abstract In this study, α-phase nucleating agent (NA) 1,3:2,4-bis(3,4-dimethylbenzylidene) sorbitol (DMDBS), β-phase rare earth NA (WBG), and their compound NAs were introduced into isotactic polypropylene (iPP) matrix, respectively. Crystallization kinetics and subsequent melting behavior of the nucleated iPPs were comparatively studied by differential scanning calorimetry (DSC) under both isothermal and nonisothermal conditions. For the isothermal crystallization process, it is found that the Avrami model successfully described the crystallization kinetics. The active energy of nonisothermal crystallization of iPP was determined by the Kissinger method and showed that the addition of nucleating agents increased the activation energy. Melting behavior and crystalline structure of the nucleated iPPs are dependent on the nature of NAs and crystallization conditions. Higher proportion of β-phase can be obtained at higher content of β-nucleating agent and lower crystallization temperature or lower cooling rate.

Keywords Crystallization kinetics · Melting behavior ·
α-Nucleating agent · β-Nucleating agent ·
Compound nucleating agents · Isotactic polypropylene

Z. Wei (✉) · W. Zhang · G. Chen · J. Liang · S. Yang
School of Automotive Engineering, Dalian University
of Technology, 116024 Dalian, China
e-mail: zywei@dlut.edu.cn

P. Wang · L. Liu (✉)
School of Transportation and Logistics Engineering,
Dalian Maritime University, 116026 Dalian, China
e-mail: lliu@newmail.dlmu.edu.cn

Introduction

Isotactic polypropylene (iPP), as one of the widely used commodity polymers, has been intensively researched in the last years because of its polymorphism characteristic (the monoclinic α-phase, the trigonal β-phase, and the orthorhombic γ-phase) [1]. Among all the crystalline forms of iPP, the monoclinic α-phase and trigonal β-phase have attracted most interest because α-phase is the most common phase in melt-crystallized samples or articles and β-phase usually shows better impact toughness and drawability than α-phase [2].

Incorporation of nucleating agents (NAs) with isotactic polypropylene (iPP) is an effective method to improve properties of iPP related to crystallization and morphology [3–11]. The most common nucleating agents are divided into α nucleating agents and β nucleating agents, in which most α nucleating agents can improve tensile and flexural properties as well as transparency of iPP, while β nucleating agents can increase impact-resistance strength and heat distortion temperature of iPP; however, β nucleating agents would decrease the stiffness of iPP [12–14].

Therefore, compounding α and β nucleating agents is an attractive strategy to produce iPP with high stiffness and toughness. It is well known that mechanical properties of semicrystalline polymers are mainly dependent on their molecular weight, the nature of the crystal phase, crystallinity, and spherulite size. It is significant to achieve this objective by examining their crystallization behavior. There are many publications on the crystallization behavior of iPP nucleated with individual α or β nucleating agents [15–23], but only a few studies on the crystallization behavior of iPP nucleated with α and β compound nucleating agents [24–28].

Zhang et al. [25, 26] reported the crystallization and melting behaviors of isotactic polypropylene (iPP) nucleated with compound nucleating agents of sodium 2,2'-methylene-bis(4,6-di-tertbutylphenyl)phosphate (NA40)/dicyclohexylterephthalamide (NABW) (weight ratio of NA40 to NABW is 1:1). Bai et al. [27, 28] introduced α-phase nucleating agent 1,3:2,4-bis(3,4-dimethylbenzylidene) sorbitol (DMDBS), β-phase nucleating agent aryl amides compound (TMB-5), and their compounds into PP matrix, and comparatively investigated the crystallization and melting of iPP nucleated by individual and compound nucleating agents. However, in such a compound system the nucleation effect and crystallization behavior of α and β nucleating agents are not yet clear.

In this study, α nucleating agent sorbitol derivatives DMDBS and β nucleating agent rare earth complex WBG were added simultaneously in iPP matrix. DMDBS and WBG are high effective nucleating agents for α-iPP and β-iPP, respectively [29–34]. The crystallization kinetics and subsequent melting behavior of iPP nucleated with individual and compound nucleating agents were comparatively investigated under both isothermal and nonisothermal conditions. The aim of this article was to understand the nucleation effect and crystallization behavior of iPP nucleated with compound nucleating agents under different crystallization processes, and affords an effective method to regulate the crystalline structure of iPP through altering the composition of compound nucleating agents.

Experimental

Materials

All the materials used in this study are commercially available. iPP (T30S, West Pacific Petrochemical Co., Dalian, China) with isotacticity index 95%, melt flow rate (MFR) of 2.5 g/10 min (230 °C/2.16 kg) was used as the matrix polymer. The α-nucleating agent 1,3:2,4-bis(3,4-dimethylbenzylidene) sorbitol (DMDBS, HX3) was supplied by Hengxin Chemical Co. (Wuhan, Hubei Province, China). The rare earth β-phase NA (WBG) was purchased from Guangdong Winner Functional Materials Co. (Foshan, Guangdong Province, China). It was a heteronuclear dimetal complex of lanthanum and calcium with some specific ligands. The WBG has a general formula of $Ca_xLa_{1-x}(LIG1)_m(LIG2)_n$, where x and $1 - x$ are the proportion of Ca^{2+} and La^{3+} ions in the complex, while LIG1 and LIG2 are, respectively, dicarboxylic acid and amide-type ligands with coordination numbers of m and n.

Sample preparation

Blends of iPP and nucleating agents were produced at 190 °C for 10 min, with a rotor speed of 60 rpm, using a HAAKE (Thermo Haake Rheomix) batch melt mixer. The iPP nucleated with 0.2 mass% HX3, 0.2 mass%WBG, 0.2 mass% HX3 + 0.2 mass%WBG were prepared and denoted as iPP1, iPP2, and iPP3, respectively. Also, a pure iPP sample was prepared with an identical mixing process and used as a control (denoted as iPP0).

X-ray diffraction

The samples were compression-molded at 190 °C under a pressure of 15 MPa for 5 min and then naturally cooled to the room temperature. X-ray diffraction (XRD) experiments were conducted with a Dmax-Ultima + X-ray diffractometer (Rigaku, Japan) (Cu K_α, $\lambda = 0.15418$ nm, 40 kV, 40 mA, reflection mode). Patterns were recorded at a scanning speed of 1.2 min^{-1} and a scanning step of 0.02° from 10° to 30°. The relative content of the β-phase, k_β, can be calculated from the XRD profiles according to Turner Jones' equation [35]:

$$k_\beta = \frac{H(\beta)}{H(\beta) + H(\alpha_1) + H(\alpha_2) + H(\alpha_3)} \times 100\% \qquad (1)$$
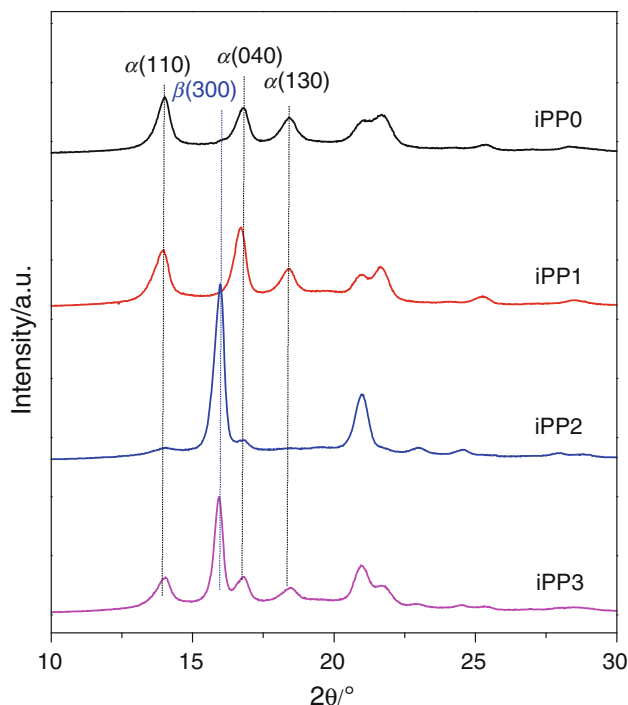
where $H(\beta)$ is the diffraction intensity of $\beta(300)$ planes at diffraction angle $2\theta = 16.0°$, $H(\alpha_1)$, $H(\alpha_2)$ and $H(\alpha_3)$ are the diffraction intensities of the $\alpha(110)$, $\alpha(040)$, and $\alpha(130)$ planes at diffraction angles $2\theta = 14.1°$, 16.9°, and 18.5°, respectively.

It has been calculated from Fig. 1 that k_β for iPP0, iPP1, iPP2, and iPP3 are 0, 0, 92, and 53%, respectively.

Differential scanning calorimetry

Isothermal and nonisothermal crystallizations were performed in a DSC1 (Mettler-Toledo, Switzerland) differential scanning calorimeter. The instrument was calibrated using high purity indium and zinc standards. Each sample (ca. 2–3 mg) was initially melted at 200 °C for 5 min to erase the previous thermal and mechanical history and then cooled rapidly to the presetting isothermal crystallization temperature (T_c). For nonisothermal crystallizations, after melting at 200 °C for 5 min the sample was cooled to 80 °C at the constant cooling rates (V_c) of 2, 5, 10, 15, 20, and 30 °C min^{-1}. After isothermal or nonisothermal crystallization, the samples were subsequently heated at 10 °C min^{-1} (V_h) to 200 °C and the heat flows during both crystallization and melting process were recorded.

DSC is an alternative to estimate the relative content of the β-phase in β-nucleated iPP [32]. The relative content of

Fig. 1 XRD patterns of iPP and nucleated iPPs

Fig. 2 Melting curve of iPP3 for determining the relative content of β-phase

$$\Delta H_\beta = \Delta H_\beta^* \times A \qquad (4)$$

$$A = \left[1 - \frac{h_2}{h_1} \right]^{0.6} \qquad (5)$$

$$\Delta H_\alpha = \Delta H_{\text{total}} - \Delta H_\beta = \Delta H_\alpha^* + \Delta H_\beta^* - \Delta H_\beta^* \qquad (6)$$

In Eq. 5, h_1 and h_2 are the heights from the base line to the β-phase peak and minimum point, respectively (Fig. 2).

Results and discussion

Isothermal crystallization kinetics

Isothermal crystallization kinetics of iPP and nucleated iPPs was performed with DSC at various crystallization temperatures. Figure 3 shows the heat flow evolution of iPP and nucleated iPPs for the isothermal crystallization obtained by rapidly cooling the molten polymer to the crystallization temperature (T_c). There is only single and symmetric exothermic peak on DSC traces of both iPP and nucleated iPPs. Furthermore, the effect of T_c on crystallization rate is clearly observed in isothermal thermograms. It was obvious that as the supercooling, i.e., the difference between the melting and crystallization temperature, decreases, the crystallization rate becomes slower and the exothermic peak becomes broader. Hence, the rate of crystallization decreases with increasing temperature.

Based on the assumption that the evolution of crystallinity is linearly proportional to the evolution of heat released during the crystallization, the relative degree of crystallinity, X_t, can be calculated by integration of the exothermal peaks from the following equation [38]:
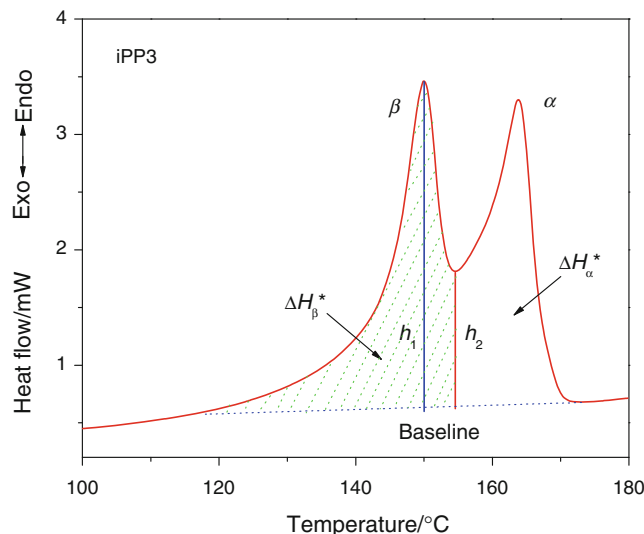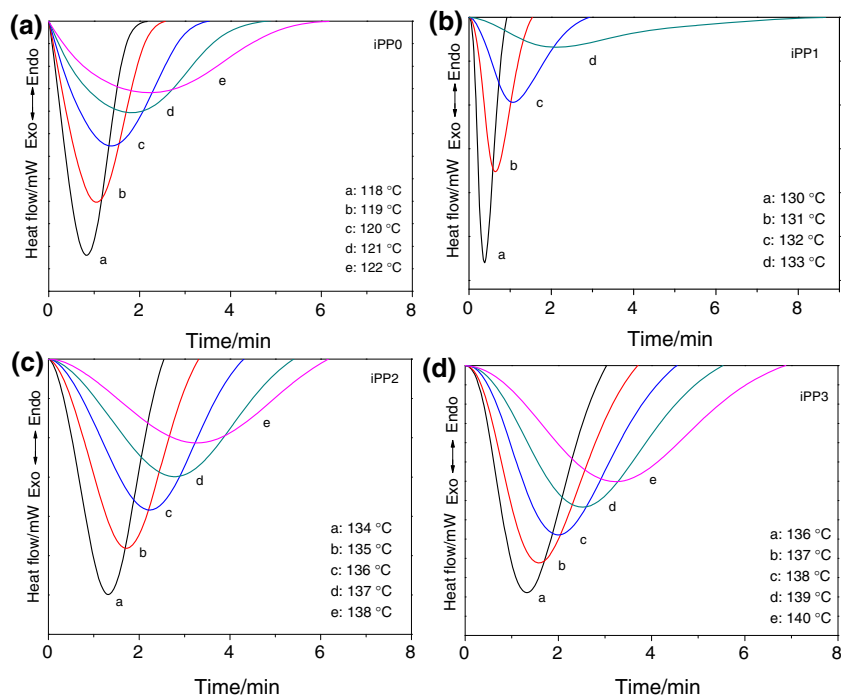
β-phase estimated by DSC melting curve could be defined as Φ_β and calculated from the following equation:

$$\Phi_\beta = \frac{X_\beta}{X_\alpha + X_\beta} \times 100\% \qquad (2)$$

where X_α and X_β are the crystallinity of the α- and β-phase, respectively, and could be calculated separately according to

$$X_i = \frac{\Delta H_i}{\Delta H_i^\circ} \times 100\% \qquad (3)$$

where ΔH_i is the calibrated enthalpy of fusion of either α- or β-phase, ΔH_i° is the standard enthalpy of fusion of α- or β-PP, being 178 and 170 J g^{-1}, respectively [36]. Overlapping of α- and β-phase peaks was often observed in the DSC melting curves, so the enthalpy of fusion for α- and β-phase were determined according to the following calibration method [37]. The total enthalpy of fusion, ΔH, was integrated from the base line to the DSC thermogram. A vertical line was drawn through the minimum between the α- and β-phase peaks and the total enthalpy of fusion was divided into β-component, ΔH_β^* and α-component, ΔH_α^*. Because the less-perfect α-crystals melt before the maximum point during heating and contributed to the ΔH_β^*, the real value of enthalpy of fusion of β-phase, ΔH_β, has been approximated by a production of multiplying ΔH_β^* with a calibration factor A [37]:

Fig. 3 Isothermal crystallization curves of iPP and nucleated iPPs at the indicated temperatures

$$X_t = \frac{X_t(t)}{X_t(\infty)} = \frac{\int_0^t (dH/dt)dt}{\int_0^\infty (dH/dt)dt} \quad (7)$$

where (dH/dt) denotes the rate of heat flow, $X_t(t)$ and $X_t(\infty)$ represent the absolute crystallinity at the elapsed time during the course of crystallization and at the end of the crystallization process, respectively.

The evolution of relative crystallinity with crystallization time at various temperatures (not shown here because of space limitations) shows the S-shaped curves, which are consistent with nucleation and growth processes. The half time of crystallization ($t_{1/2}$) obtained from these curves is frequently used to evaluate the rate of crystallization of iPP. The shorter the $t_{1/2}$ is, the higher the crystallization rate. From the data summarized in Table 1, it seems that the $t_{1/2}$ values increase almost exponentially as the crystallization temperature is increased.

The Avrami method is the most common approach for analysis of isothermal crystallization according to the following equations [39–41]:

$$X_t = 1 - \exp(-Z_t t^n) \quad (8)$$

$$\ln[-\ln(1 - X_t)] = \ln Z_t + n\ln t \quad (9)$$

where n is the Avrami exponent, which is relevant to the mechanism of nucleation, and Z_t is the overall crystallization rate constant, which is dependent on nucleation and crystal growth.

The Avrami plots for the iPP nucleated with α/β compound nucleating agents obtained at various temperatures are illustrated in Fig. 4. There are good linearities of

Table 1 Isothermal crystallization kinetics data of iPP and nucleated iPPs

Sample	$T_c/°C$	$t_{1/2}/min$	n	Z_t/min^{-n}	n (average)
iPP0	118	0.855	2.26	0.981	2.05
	119	1.061	2.17	0.591	
	120	1.441	2.01	0.329	
	121	1.899	1.92	0.203	
	122	2.359	1.89	0.136	
iPP1	130	0.422	3.11	10.681	2.79
	131	0.703	2.98	1.994	
	132	1.218	2.69	0.414	
	133	2.781	2.39	0.061	
iPP2	134	1.316	2.77	0.319	2.76
	135	1.713	2.77	0.154	
	136	2.224	2.78	0.075	
	137	2.776	2.72	0.043	
	138	3.246	2.75	0.027	
iPP3	136	1.432	2.97	0.243	2.91
	137	1.714	2.88	0.149	
	138	2.138	2.95	0.075	
	139	2.640	2.90	0.042	
	140	3.339	2.87	0.022	

$\ln[-\ln(1 - X_t)]$ versus $\ln t$ in a wide relative crystallinity range. It can be concluded that the Avrami equation is quite successful for analyzing the experimental data of the isothermal crystallization kinetics. The parameters of Z_t and n, which are obtained from the plots of $\ln[-\ln(1 - X_t)]$ versus $\ln t$, are listed in Table 1. The Avrami parameter Z_t is

Fig. 4 Avrami plots of $\ln[-\ln(1 - X_t)]$ versus $\ln t$ for iPP and nucleated iPPs
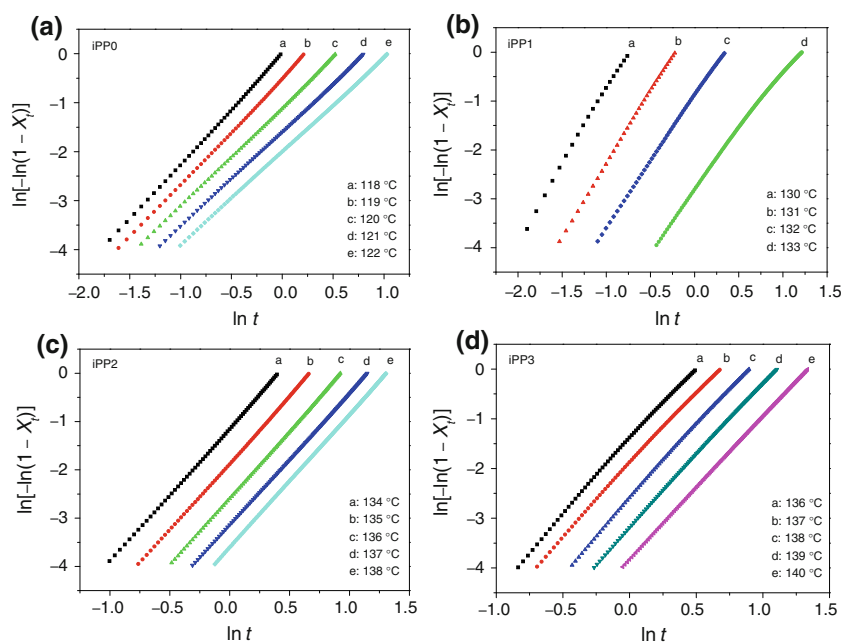
indicative of the crystallization rate. As expected, Z_t decreases with the increase in crystallization temperature.

It is known that Avrami exponent n strongly depends on both the mechanism of nucleation and the morphology of crystal growth. For pure iPP, an average value of $n = 2.05$ is obtained over the crystallization temperature range studied, which is close to the results reported in the literature [32, 42]. The result indicates that it may be related with a heterogeneous nucleation followed by two-dimensional or lamellar growth due to the existence of impurities and catalyst residues [9]. While for iPP nucleated with individual and compound nucleating agents, the average values of n are close to 3, which is a heterogeneous nucleation followed by three-dimensional spherulite growth. The above results indicate that the addition of nucleating agents can change the crystal growth patterns of iPP.

Nonisothermal crystallization and activation energy

From a technological point of view, nonisothermal crystallization conditions approach more closely the industrial conditions of polymers processing; it is of great practical importance to understand the crystallization of polymers under nonisothermal conditions. The nonisothermal crystallization of iPP and nucleated iPPs was carried out by DSC with cooling rates from 2 to 30 °C min^{-1}. The thermograms of iPP and nucleated iPPs are reported in Fig. 5. It should be noticed that the crystallization curves of β-nucleated blends (iPP2 and iPP3) showed simultaneous crystallization of the α- and β-phase of iPP, since only a single exothermic peak in spite of the formation of two

separate polymorphic phases. With increasing cooling rate, crystallization peak temperature (T_p) of iPP shifts to lower temperature. Especially, the corresponding crystallization peak temperatures (T_p) at different cooling rates were determined from the cooling curves, and the results are shown in Fig. 6. For all the samples, the T_p decreases with increasing cooling rate. It is evident that the crystallization temperature is affected by the cooling rate: the lower the cooling rate, the higher the crystallization peak temperature. Furthermore, it can be recognized that, at the same cooling rates, T_p of nucleated iPP is greatly increased compared with that of iPP.

At lower cooling rate (<10 °C min^{-1}), there is undistinguishable between T_p of iPP nucleated with compound NAs and those of iPP nucleated with individual NAs. However, at higher cooling rate (>10 °C min^{-1}), their discrepancy is remarkable and shows a tendency to enlarge. The results indicate that combining the α/β compound NAs is favorable for crystallization starting at higher temperature.

The Kissinger's method has been widely applied to evaluate the overall effective activation energy by considering the variation of the crystallization peak temperature with the cooling rate [43].

$$\frac{d\left(\ln\frac{\Phi}{T_p^2}\right)}{d\left(\frac{1}{T_p}\right)} = -\frac{\Delta E}{R} \tag{10}$$

where Φ is cooling rate, T_p is the crystallization peak temperature, and R is the gas constant, ΔE is the activation energy of nonisothermal crystallization.
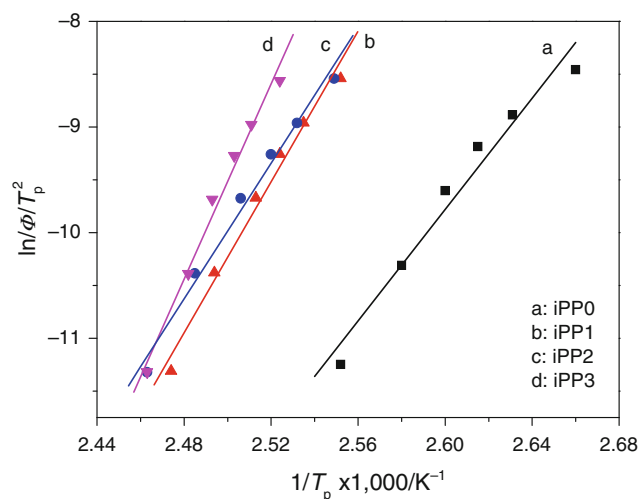
The activation energy of nonisothermal crystallization (ΔE) is calculated from the slope of $\ln\Phi/T_p^2$ versus $1/T_p$. As

Fig. 5 Nonisothermal
crystallization curves of iPP
and nucleated iPPs at various
cooling rates
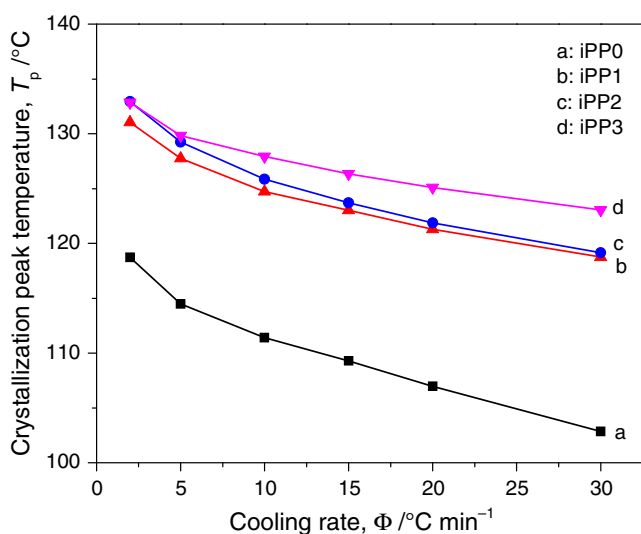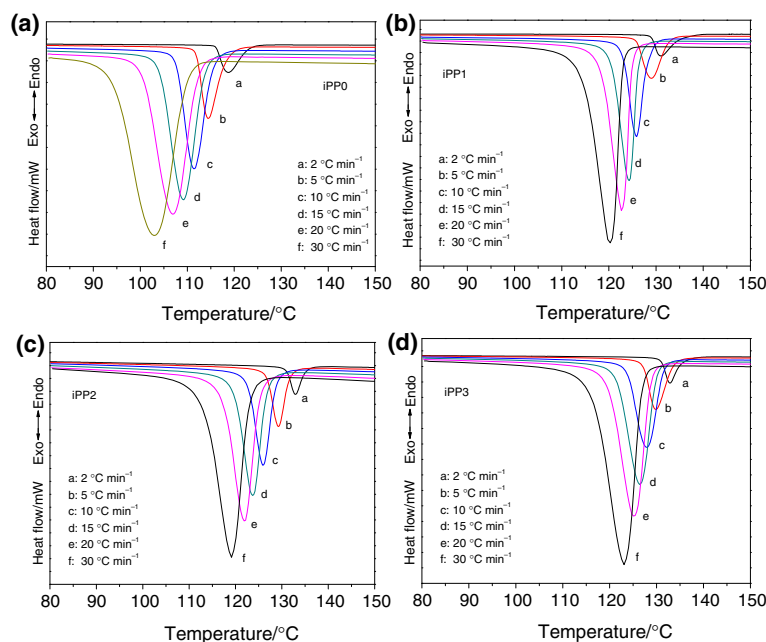
Fig. 6 Crystallization peak temperature (T_p) of iPP and nucleated iPPs at various cooling rates

Fig. 7 Plots of $\ln(\Phi/T_p^2)$ versus $1/T_p$ to determine the activation energy of nonisothermal crystallization of iPP and nucleated iPPs

shown in Fig. 7, the ΔE of iPP0, iPP1, iPP2, and iPP3 during nonisothermal crystallization is determined to 216, 297, 260, and 344 kJ mol^{-1}, respectively. It can be seen that addition of β-NA WBG increases slightly the crystallization activation energy of iPP; however, the ΔE of iPP nucleated with α-NA DMDBS and α/β compound NAs is considerably higher than that of pure iPP. From the kinetic viewpoint, the activation energy could be correlated with the crystallization rate. Generally, high crystallization activation energy would hinder the crystallization and result in the decrease of crystallization rate. However, an

opposite phenomenon is observed in our study. It seems that addition of NAs increases the crystallization activation energy of iPP, but, as discussion earlier, it increases the crystallization rate. The similar results were reported for other nucleating agents by several researchers [9, 18].

The reason for this contradiction is the dual effect of nucleating agents on crystallization of iPP. On the one hand, nucleating agents may hinder the transfer of macromolecular segments from iPP melts to the crystal growth surface due to the strong interaction between nucleating agents and segments of iPP, which leads to the increase of ΔE; on the other hand, nucleating agents serve as

heterogeneous nuclei and favor crystallization growth of molecular in interface, which accelerates greatly the nucleation rate. Among the crystallization processes consisting of nucleation and growth, nucleation is the controlling step during crystallization, and the increasing of nucleation rate results in the increase of the total crystallization rate and crystallization temperature.

Melting behavior

After isothermal and nonisothermal crystallization, the subsequent melting behavior of pure iPP and nucleated iPPs was investigated by DSC at heating rate of 10 °C min^{-1}. As expected, the melting profile of pure iPP and iPP nucleated with DMDBS mainly shows the endotherm referring to α-phase, which means almost only α-phase appeared in iPP after isothermally crystallized at the whole T_c range adopted in this work. However, for WBG-nucleated iPP, as shown in Fig. 8a, a main melting peak at 153–158 °C and a subsequent shoulder peak are observed. These two melting peaks are corresponding to the enthalpy of fusion of β-phase and β-α recrystallization. During the heating process, the unstable β-phase tends to melt first and recrystallize as α-phase with more stable crystalline structure. The melting peak temperature of β-iPP increases with the increase of crystallization temperature. This fact might be explained by thermodynamic cause [26]. The most important thermodynamic parameter of the crystallization is the undercooling ΔT ($\Delta T = T_m^0 - T_c$), which shows how far the polymer crystallizes from its melt crystal equilibrium state. The lower the undercooling, the more perfect the crystals are formed and hence, the higher the crystallinity, the higher the melting temperature.
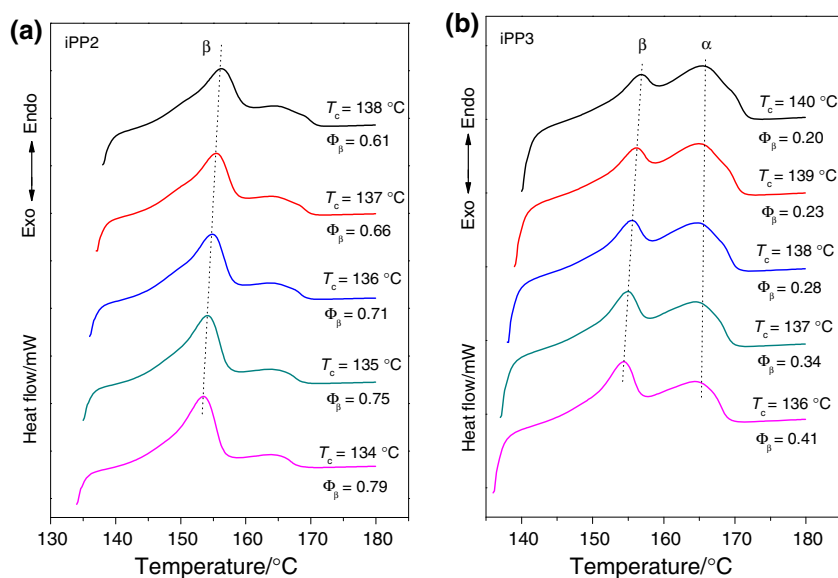
There are two obvious melting peaks (Fig. 8b), which appear at about 153 and about 164 °C, respectively. These two melting peaks correspond to the characteristic peaks of β-phase and α-phase, respectively, which means that these compound NAs can induce iPP to form both α-crystals and β-crystals. It is well known that higher crystallization temperature is unfavorable for the formation of the β-phase [2]. According to the above-mentioned calculated method, the relative content of β-phase, Φ_β, in PP3 sample as well as PP2 sample decreases with the increase of crystallization temperature.

The DSC heating curves of iPP nucleated by different NAs after nonisothermal crystallization at different cooling rates. For pure iPP and DMDBS-nucleated iPP, there is only one melting peak at about 161–165 °C, corresponding to the melting of α-phase. For WBG-nucleated iPP as shown in Fig. 9a, multiple melting peaks are observed at approximate 148–156, 157–165, and 166–170 °C (shown as β, α_1, and α_2, respectively), indicating the melting of β-phase and α-phase [27]. With increasing of cooling rate, the melting peak of β-phase shifts to lower temperature, a shoulder melting peak (α_2) presents at higher temperature and becomes more apparent above cooling rate of 10 °C min^{-1}; furthermore, at cooling rate of 30 °C min^{-1}, the main peak of β-phase splits into two peaks, that is, a new shoulder peak (β_2) appears in the DSC heating curve. However, the melting peak of α_1 keeps nearly invariant. It can be deduced that the melting peak α_1 is associated with the fusion of α-phase formed during the nonisothermal crystallization process, and melting peak α_2 is contributed to the fusion of reorganized α-phase from the melting of β-phase during the heating process.

The melting behavior of iPP3 nucleated with compound NAs is dependent on the cooling rate (Fig. 9b). The

Fig. 8 Melting curves of iPP2 and iPP3 after isothermal crystallization at the indicated temperatures

Fig. 9 Melting curves of iPP2 and iPP3 after nonisothermal crystallization at different cooling rates
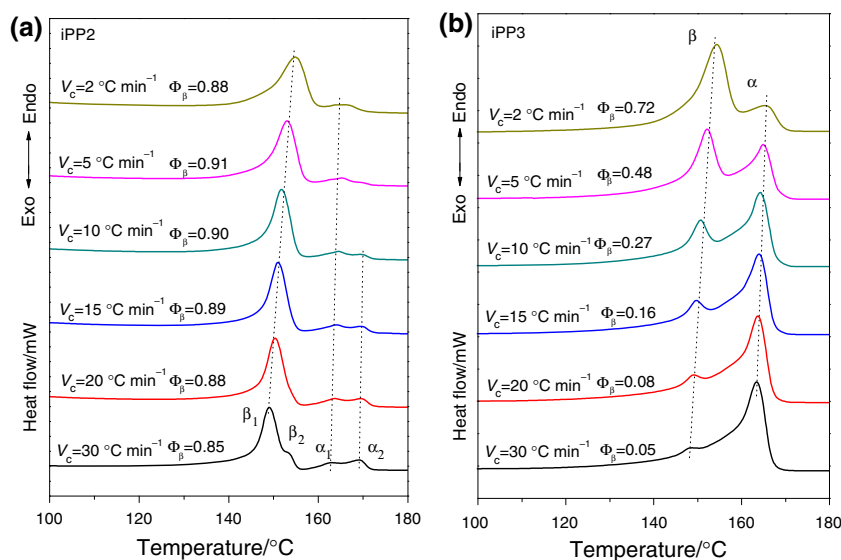
relative content of β-phase in iPP3 sample decreases with the increase of crystallization temperature. The lower the cooling rate is, the higher the proportion of the β form will be, especially for iPP3. During the nonisothermal crystallization of iPP3, when the cooling rate is low, crystallization occurs in a higher temperature region in which the self-nucleation of iPP is difficult to initiate; α-crystals are suppressed, while the nucleating agent WBG can effectively provide a large number of foreign nuclei to induce the formation of the β form. On the contrary, at a high cooling rate, crystallization occurs in a lower temperature region in which the α-nucleation of iPP is predominant, and this could result in the main α form. Therefore, higher percent of the β phase can be obtained at lower cooling rate.

Conclusions

The crystallization kinetics and sequential melting behavior of iPP nucleated with individual nucleating agent and compound nucleating agents were comparatively investigated under isothermal and nonisothermal conditions. It is found that the Avrami model successfully describes the kinetics data of the isothermal crystallization process. The obtained Avrami exponent indicated that addition of nucleating agents changes the crystal growth pattern of iPP. Furthermore, the addition of nucleating agents increases the crystallization activation energy. Melting behavior and crystalline structure of the nucleated iPP are dependent on both the nature of α/β nucleating agents and crystallization process. Moreover, lower crystallization temperature and lower cooling rate are favorable for the formation of β-crystals. Therefore, higher proportion of β-phase can be

obtained at higher content of β-nucleating agent and lower crystallization temperature or lower cooling rate.

References

1. Varga J. Supermolecular structure of isotactic polypropylene—review. J Mater Sci. 1992;27:2557–79.
2. Varga J. β-Modification of isotactic polypropylene: preparation, structure, processing, properties, and application. J Macromol Sci: Phys. 2002;41B:1121–71.
3. Libster D, Aserin A, Garti N. Advanced nucleating agents for polypropylene. Polym Adv Technol. 2007;18:685–95.
4. Nagarajan K, Levon K, Myerson AS. Nucleating agents in polypropylene. J Therm Anal Calorim. 2000;59:497–508.
5. Kristiansen M, Werner M, Tervoort T. The binary system isotactic polypropylene/bis(3,4-dimethylbenzylidene)sorbitol: phase behavior, nucleation, and optical properties. Macromolecules. 2003;36:5150–6.
6. Blomenhofer M, Ganzleben S, Hanft D. "Designer" nucleating agents for polypropylene. Macromolecules. 2005;38:3688–95.
7. Varga J, Menyhárd A. Effect of solubility and nucleating duality of N′N″-dicyclohexyl-2, 6-naphthalene-dicarboxamide on the supermolecular structure of isotactic polypropylene. Macromolecules. 2007;40:2422–31.
8. Zhang YF, Xin Z. Effects of substituted aromatic heterocyclic phosphate salts on properties, crystallization, and melting behaviors of isotactic polypropylene. J Appl Polym Sci. 2006;100:4868–74.
9. Zhang YF, Xin Z. Isothermal and nonisothermal crystallization kinetics of isotactic polypropylene nucleated with substituted aromatic heterocyclic phosphate salts. J Appl Polym Sci. 2006;101:3307–16.
10. Menyhárd A, Varga J, Molnár G. Comparison of different β-nucleators for isotactic polypropylene, characterisation by DSC

and temperature-modulated DSC (TMDSC) measurements. J Therm Anal Calorim. 2006;83:625–30.

11. Jana V, Veronika H, Obadal M. Crystallization of polypropylene with a minute amount of β-nucleator. J Therm Anal Calorim. 2006;86:687–91.

12. Karger-Kocsis J, Varga J. Effects of beta alpha transformation on the static and dynamic tensile behavior of isotactic polypropylene. J Appl Polym Sci. 1996;62:291–300.

13. Karger-Kocsis J, Varga J, Ehrenstein GW. Comparison of the fracture and failure behaviour of injection molded alpha- and beta-polypropylene in high-speed three-point bending tests. J Appl Polym Sci. 1997;64:2059–66.

14. Menyhárd A, Gahleitner M, Varga J, Bernreitner K, Jääskeläinen P, Oysad H, et al. The influence of nucleus density on optical properties in nucleated isotactic polypropylene. Eur Polym J. 2009;45:3138–48.

15. Menyhárd A, Faludi G, Varga J. β-Crystallisation tendency and structure of polypropylene grafted by maleic anhydride and its blends with isotactic polypropylene. J Therm Anal Calorim. 2008;93:937–45.

16. Zhang ZS, Wang CG, Yang ZG. Crystallization behavior and melting characteristics of PP nucleated by a novel supported β-nucleating agent. Polymer. 2008;49:5137–45.

17. Li C, Isshiki N, Saito H. Nucleation effect of cyclodextrin inclusion compounds on the crystallization of polypropylene. J Polym Sci Part B: Polym Phys. 2009;47:130–7.

18. Zhao SC, Zhi C, Xin Z. A highly active novel β-nucleating agent for isotactic polypropylene. Polymer. 2008;49:2745–54.

19. Dong M, Gu ZX, Yu J, Su ZQ. Crystallization behavior and morphological development of isotactic polypropylene with an aryl amide derivative as β-form nucleating agent. J Polym Sci: Polym Phys. 2008;46:1725–33.

20. Dong M, Guo ZX, Su ZQ, Yu J. Study of the crystallization behaviors of isotactic polypropylene with sodium benzoate as a specific versatile nucleating agent. J Polym Sci: Polym Phys. 2008;46:1183–92.

21. Wang JB, Dou Q. Nonisothermal crystallization kinetics and melting behaviors of isotactic polypropylene/N,N′,N″-tris-tertbutyl-1,3,5-benzene-tricarboxamide. J Macromol Sci: Phys. 2008;47B:629–42.

22. Wang JD, Dou Q. Crystallization behaviors and optical properties of isotactic polypropylene: comparative study of a trisamide and a rosin-type nucleating agent. Colloid Polym Sci. 2008;286:699–705.

23. Liu MX, Guo BC, Du ML, Chen F, Jia DM. Halloysite nanotubes as a novel β-nucleating agent for isotactic polypropylene. Polymer. 2009;50:3022–30.

24. Menczel J, Varga J. Influence of nucleating agents on crystallization of polypropylene. 1. Talc as a nucleating agent. J Therm Anal. 1983;28:161–74.

25. Zhang YF, Xin Z. Isothermal crystallization behaviors of isotactic polypropylene nucleated with α/β compounding nucleating agents. J Polym Sci: Polym Phys. 2007;45:590–6.

26. Zhang YF. Crystallization and melting behaviors of isotactic polypropylene nucleated with compound nucleating. J Polym Sci: Polym Phys. 2008;46:911–6.

27. Bai HW, Wang Y, Liu L, Zhang J, Han L. Nonisothermal crystallization behaviors of polypropylene with α/β nucleating agents. J Polym Sci B: Polym Phys. 2008;46:1853–67.

28. Bai HW, Wang Y, Zhang Q, Liu L, Zhou W. A comparative study of polypropylene nucleated by individual and compounding nucleating agents. I. Melting and isothermal crystallization. J Appl Polym Sci. 2009;111:1624–37.

29. Smith TL, Masilamani D, Bui LK. The mechanism of action of sugar acetals as nucleating agents for polypropylene. Macromolecules. 1994;27:3147–55.

30. Kristiansen M, Tervoort T, Smith P. Mechanical properties of sorbitol-clarified isotactic polypropylene: influence of additive concentration on polymer structure and yield behavior. Macromolecules. 2005;38:10461–5.

31. Zhang YF, Li X, Wei XS. Non-isothermal crystallization kinetics of isotactic polypropylene nucleated with 1,3:2,4-bis(3,4-dimethylbenzylidene) sorbitol. J Therm Anal Calorim 99(3). doi:10.1007/s10973-009-0372-1.

32. Xiao WC, Wu PY, Feng JC. Effect of β-nucleating agents on crystallization and melting behavior of isotactic polypropylene. J Appl Polym Sci. 2008;108:3370–9.

33. Xiao WC, Wu PY, Feng JC, Yao RY. Influence of a novel β-nucleating agent on the structure, morphology, and nonisothermal crystallization behavior of isotactic polypropylene. J Appl Polym Sci. 2009;111:1076–85.

34. Xu L, Xu K, Chen H, Zheng Q, Liu F, Chen M. Thermal behavior of isotactic polypropylene in different content of β-nucleating agent. J Therm Anal Calorim. 2009;96:733–40.

35. Turner Jones A, Aizelwood JM, Beckett DR. Crystalline forms of isotactic polypropylene. Makromol Chem. 1964;75:134–58.

36. Li JX, Cheung WL, Jia DM. A study on the heat of fusion of β-polypropylene. Polymer. 1999;40:1219–22.

37. Li JX, Cheung WL. A correction function to determine the β-fusion heat in a mixture of α- and β-PP. J Therm Anal Calorim. 2000;61:757–62.

38. Vilanova PC, Ribas SM, Guzman GM. Isothermal crystallization of poly(ethylene-terephthalate) of low molecular weight by differential scanning calorimetry: 1. Crystallization kinetics. Polymer. 1985;26:423–8.

39. Avrami M. Kinetics of phase change. I. General theory. J Chem Phys. 1939;7:1103–12.

40. Avrami M. Kinetics of phase change. II. Transformation-time relations for random distribution of nuclei. J Chem Phys. 1940;8:212–24.

41. Avrami M. Kinetics of phase change. III. Granulation, phase change, and microstructure. J Chem Phys. 1941;9:177–84.

42. Huang JW. Dispersion, crystallization kinetics, and parameters of Hoffman-Lauritzen theory of polypropylene and nanoscale calcium carbonate composite. Polym Eng Sci. 2009;49:1855–64.

43. Kissinger HE. The crystallization kinetics with heating rate in differential thermal analysis. J Res Natl Bur Stand. 1956;57:217–21.